Swarm and Evolutionary Computation 11 (2013) 46–54

Contents lists available at SciVerse ScienceDirect

Swarm and Evolutionary Computation

journal homepage: www.elsevier.com/locate/swevo

Regular Paper

Leukocyte segmentation in tissue images using differential evolution algorithm

Mukesh Saraswat*, K.V. Arya, Harish Sharma

ABV-Indian Institute of Information Technology and Management, Gwalior, India

ARTICLE INFO

Article history:
Received 16 June 2012
Received in revised form
5 December 2012
Accepted 16 February 2013
Available online 28 February 2013

Keywords:
Nuclei
Image segmentation
Multi-level threshold
Differential evolutionary algorithms

ABSTRACT

An automatic segmentation of leukocytes can assist pharmaceutical companies to take decisions in the discovery of drugs and encourages for development of automated leukocyte recognition system. Segmentation of leukocytes in tissue images is a complex process due to the presence of various noise effects, large variability in the images and shape of the nuclei. Surprisingly, rare efforts have been made to automate the segmentation of leukocytes in various disease models on hematoxylin and eosin (H&E) stained tissue images. The present work proposes a novel strategy based on differential evolution (DE) algorithm to segment the leukocytes from the images of mice skin sections stained with H&E staining and acquired at 40 × magnification. The proposed strategy is a first inline report used in such type of image database. Further, the proposed strategy is compared with well-known segmentation algorithms. The results show that the proposed strategy outperforms the traditional image segmentation techniques.

© 2013 Elsevier B.V. All rights reserved.

1. Introduction

Inflammation is a complex protective reaction where injurious agents are either destroyed, diluted or walled-off [1]. Inflammation nearly occurs in every known disease at some time in their course. A controlled inflammatory reaction is a part of protective mechanism; however, in many instances identification and removal of inflammation are not achieved. This reaction is very deleterious. A number of anti-inflammatory drugs are available [2] but due to their reported harmful side effects in recent posts, some of them are banned in market for further use (e.g. Rofecoxib). Thus still there is a challenge for scientists to discover anti-inflammatory drugs with minimal side effects.

Inflammation has two phases: exudative (acute inflammation phase) and cellular (sub-acute or chronic phase) [1]. A variety of instruments are available to aid automation of acute inflammatory reactions for reducing human subjectivity and workload. However, rare work have been done in the quantification of inflammatory cells in the tissue images due to their wide natural biological variability. Recently, we have noticed articles on chicken skin model [2], mice skin model [3], air pouch model [4], etc. where inflammatory cells (leukocytes) were quantified manually. Manual counting of leukocytes is a time consuming process and requires a trained dedicated pathologist. The number of variables such as chances of biasness and variations in staining characteristics pose challenges for the research scientists in counting leukocytes manually [5,6]. Therefore, to reduce these problems, there has been a growing interest in developing tools for quantification of leukocytes using image processing techniques. Image processing techniques are widely used in the field of medical imaging, computer vision, security, etc. [7–9]. Therefore, it is interesting to use the image processing techniques for quantifying the leukocytes. Some useful algorithms have already been developed for separation of leukocytes in blood smears [10,11] but rare efforts have been made for tissue section images [6] due to their complex structural morphology.

Leukocytes consist of nucleus (bluish color when stained with hematoxylin and eosin (H&E) staining) within cytoplasm (pinkish color). Leukocyte can be identified with the structural and textual information of its nucleus and cytoplasm. Therefore, nuclei and cytoplasm segmentation have vital importance in leukocytes identification system. Automation of leukocytes segmentation faces a set of challenges such as shape and size variability and presence of different artifacts [5,6], etc. Further, the tissue images stained with H&E staining make the segmentation process more complex. Therefore, considering the above limitations, a novel leukocytes segmentation strategy for images of inflamed mice skin section stained with H&E staining and acquired at 40 × magnification using differential evolution (DE) algorithm is proposed.

DE [12] is an evolutionary algorithm (EA) and has a vital difference from other evolutionary techniques like genetic

* Corresponding author. Tel.: +91 8989474947.
E-mail addresses: saraswatmukesh@gmail.com, saraswatmukesh@iiitm.ac.in (M. Saraswat), kvarya@gmail.com (K.V. Arya), harish.sharma0107@gmail.com (H. Sharma).

2210-6502/$ - see front matter © 2013 Elsevier B.V. All rights reserved.
http://dx.doi.org/10.1016/j.swevo.2013.02.003

algorithms (GA) [13]. DE has a prime ability to explore the large search spaces efficiently. Two major advantages of DE are that it has a faster convergence rate as compare to other evolutionary algorithms and requires to adjust a few parameters due to which it can be implemented easily [14]. Recently, Das and Suganthan [15] presented state-of-the-art of DE and its major variants along with its applicability to a larger set of applications. During the last decade, the different variants of DE includes JADE [16], SaDE [17], DEGL [18], jDE [19], etc. Recently, Islam et al. [20] proposed MDE_*p*BX and observed that by applying proposed modification, the ability of DE can be improved for finding a solution in a given search space. Furthermore, the solution search capability of advance DE variants, like jDE and JADE, can also be enhanced by incorporating their proposed mutation, crossover, and parameter adaptation schemes.

Vesterstrom and Thomsen [21] observed that DE outperforms particle swarm optimization (PSO), and EAs regarding their general applicability as numerical optimization techniques using 34 widely used benchmark problems. Price et al. [12,14] compared DE with simulated annealing, variants of GA, and other evolutionary programming and observed that DE is more accurate and efficient. Hammouche et al. [22] presented a comparison among six meta-heuristic techniques namely GA, PSO, DE, ant colony optimization (ACO), simulated annealing (SA), and tabu search to solve the multilevel threshold problem of image processing and found that DE provides the most efficient quality solutions. Osuna-Enciso et al. [23] presented an empirical comparison of three state-of-the-art-nature inspired algorithms, PSO, artificial bee colony (ABC), and DE to perform image threshold by a mixture of Gaussian functions. They used statistical analysis tools to compare the results and concluded that DE not only shows a superior performance in minimizing the Hellinger distance between the original and the candidate histogram but also performs minimization in less number of evaluations for the mentioned distance cost function. Iwan et al. [24] presented a comparative study for min–max constrained optimization using PSO and DE using some selected standard benchmark functions and observed that DE outperforms PSO in terms of repeatability and quality of obtained solutions. Das et al. [25] showed the superiority of DE by extensively comparing the automatic clustering DE (ACDE) with two other state-of-the-art automatic clustering techniques based on GA and PSO. Further, DE has been successfully applied to a diverse set of optimization problems [26–32].

Therefore, this paper presents a novel leukocytes segmentation method based on differential evolution (DE) which extracts out the leukocytes from the images of inflamed mice skin section stained with H&E staining and acquired at 40 × magnification. The results are compared with well-known segmentation algorithms used by different researchers for leukocyte segmentation namely *K*-means [33], expectation–maximization (EM) algorithm [34], Fuzzy *c*-means [35] and Otsu's threshold [36].

Rest of the paper is organized as follows. Section 2 describes the problem formulations and its description. The differential evolution algorithm (DE) is explained in Section 3. The proposed segmentation strategy is described in Section 4. In Section 5, experiments are performed to compare the performances of the proposed strategy with traditional well know strategies. Finally, in Section 6, paper is concluded along with discussion.

2. Problem description

The image segmentation is a process of partitioning an image into multiple regions based on selected image properties like color, area, shape, etc. In this paper, we are dealing with the problem of automated segmentation of leukocytes in mouse skin section images stained with H&E staining. Segmentation of leukocytes in tissue images is a complex process due to the presence of various staining, illumination, and structural variability along with different artifacts/noise. Therefore, to segment these complex images, the use of multilevel image segmentation is appropriate as compare to single level. In this paper, a multilevel image segmentation technique has been introduced based on differential evolution (DE) algorithm [12].

DE [12,37] has successfully been applied to the applications of image segmentation [38] and pattern recognition [39]. This paper describes the use of DE algorithm for segmenting the leukocytes from the images of inflamed mice skin section stained with H&E staining. Since the preparation of a glass slide of tissue section undergoes various processing phases like sectioning, staining, etc., some artifacts/noise may be introduced in the slide that need to be differentiated from the leukocytes. These artifacts/noise are also visible in the microscope and have almost similar intensity as that of leukocytes. These unwanted objects could only be distinguished from the leukocytes on the basis of nucleus and cytoplasm features not by their intensity. Therefore, in the proposed mechanism, the leukocytes segmentation is done in two phases. In the first phase, objects of interest are segmented from photomicrographs of inflamed mice skin using pixel intensity information. These set of objects may also contain artifacts which are minimized in the subsequent phase. In the second phase, segmentation is based on the feature set (area of cell, eccentricity of cell, ratio of cytoplasm area to nucleus area, solidity of nucleus) of the extracted objects. The algorithm made no priori assumptions about the size, shape, texture or spatial distribution of the leukocytes.

The problem of leukocytes segmentation can be treated as an optimization problem defined by an appropriate objective function. The objective functions designed to solve this type of complex problems are generally complex, multimodal, and combinatorial and cannot be bounded by mathematical forms. Therefore, the application of several traditional strategies becomes limited. Meta-heuristic techniques are not bounded by these restrictions and hence can be a better choice to solve these types of problems. The formation of the objective functions to deal with both the segmentation phases for the proposed strategy are described in following sections.

2.1. Intensity based segmentation

The mathematical formulation of the intensity based segmentation technique is inspired by the strategy presented in [40]. Let a given RGB image, having N number of pixels, consists of L intensity levels ($\{0,1,2,\ldots,L-1\}$) for each RGB plane and n_i represents the number of pixels of intensity level i. Then, the probability of an occurrence of a pixel of intensity level i in the image, also known as probability distribution (p_i), is given as

$$p_i = \frac{n_i}{N}, \quad 0 \le i \le L-1. \tag{1}$$

The mean intensity of each RGB plane of the image is determined by the following equation:

$$\mu = \sum_{i=1}^{L} i p_i. \tag{2}$$

To classify the pixels of the image into n classes $\{D_1,D_2,\ldots,D_n\}$, $n-1$ thresholds $(t_1,t_2,\ldots,t_{n-1})$ are to be generated as expressed in

the following equation:

$$f(x,y)=\begin{cases}0, & f(x,y)\le t_1\\ \frac{t_1+t_2}{2}, & t_1<f(x,y)\le t_2\\ & \cdot\\ & \cdot\\ & \cdot\\ \frac{t_{n-2}+t_{n-1}}{2}, & t_{n-2}<f(x,y)\le t_{n-1}\\ L-1, & f(x,y)>t_{n-1}\end{cases} \quad (3)$$

where $f(x,y)$ represents the intensity value of the image of size $M\times N$ at pixel location (x,y). The class $D_j, 1\le j\le n$ contains all pixels having intensities greater than t_{j-1} and less than equals to t_j. The probability of occurrence of class D_j for each plane is given by the following equation:

$$w_j=\sum_{i=t_{j-1}+1}^{t_j} p_i. \quad (4)$$

The mean of class D_j can be calculated as follows:

$$\mu_j=\sum_{i=t_{j-1}+1}^{t_j} ip_i/w_j. \quad (5)$$

The inter-class variance can be generally defined as

$$\sigma^2=\sum_{j=1}^{n} w_j(\mu_j-\mu)^2. \quad (6)$$

To classify the different pixels based on intensity into their respective class for individual planes, the between class variance shown in Eq. (6) should be maximized. Therefore, the objective function for the proposed strategy is to maximize the three fitness functions one for each plane which is defined as

$$\phi=\max_{1<t_1<\ldots<t_{n-1}<L}\{\sigma^2(t)\}. \quad (7)$$

2.2. Features based segmentation

Let there be N number of objects which are extracted from the intensity based segmentation for a given image. Each object is represented by four features namely area of cell, eccentricity of cell, ratio of cytoplasm area to nucleus area and solidity of nucleus where the value of each feature has been scaled in [0, L–1]. The probability distribution of each feature can be defined as follows:

$$p_i=\frac{O_i}{N}. \quad (8)$$

where i represents the ith feature value, i.e., $0\le i\le L-1$, and O_i denotes the total number of objects with ith feature value.

The total mean of each feature for the image can be easily calculated as shown in Eq. (2). Further, the use of $n-1$ threshold levels has been performed as Eq. (3) and the probability of occurrence of class D_j is given by Eq. (4). Further, the mean of each class can be calculated respectively for each feature by using Eq. (5) and the between-class variance can be defined as in Eq. (6).

To classify the different objects based on feature set into their respective class, the inter-class variance represented by Eq. (6) should be maximized for each feature value. Therefore, the objective function for the proposed strategy is to maximize the four fitness functions, where one fitness function represents one feature of the object, defined as

$$\phi=\max_{1<t_1<\ldots<t_{n-1}<L}\{\sigma^2(t)\}. \quad (9)$$

The computational complexity of this optimization problem increases as the number of threshold levels increase. Many methods have been proposed in literature [41] regarding this problem. However, more recently, biologically inspired methods have been used as computationally efficient alternatives to analytical methods to solve optimization problems [38]. In this paper, we used the differential evolution (DE) [12] algorithm to solve the aforementioned optimization problem. The following section presents the DE used in this work.

3. Differential evolution algorithm

Differential evolution (DE) algorithm is relatively a simple, fast and population based stochastic search technique [12]. DE falls under the category of evolutionary algorithms (EAs). But in some sense, it differs significantly from EAs, e.g. trial vector generation process uses the information of distance and direction from current population to generate a new trial vector. Furthermore, in EAs, crossover is applied first to generate a trial vector, which is then used within the mutation operation to produce one offspring while, in DE, mutation is applied first and then crossover [42]. DE has several strategies based on method of selecting the target vector, the number of difference vectors used, and the type of crossover [12]. In this paper *DE/rand/1/bin* scheme is used where DE stands for differential evolution, 'rand' specifies that the target vector is selected randomly, '1' is for number of differential vectors, and 'bin' notation is for *binomial* crossover. The popularity of DE is due to its applicability to a wider class of problems and ease of implementation. DE consists of the properties of both evolutionary algorithm and swarm intelligence. The detailed description of DE is as follows.

Like other population based search algorithms, DE also searches the solution using a population of potential solutions (individuals). In a D-dimensional search space, an individual is represented by a D-dimensional vector $(x_{i1},x_{i2},\ldots,x_{iD})$ where $i=1,2,\ldots,NP$ and NP is the population size (number of individuals).

In DE, there are three operators: mutation, crossover and selection. Initially, a population is generated randomly with uniform distribution then the mutation, crossover and selection operators are applied to generate a new population. Offspring vector generation is a crucial step in DE process. The two operators, mutation and crossover, are used to generate the offspring vectors. The selection operator is used to select the best vector between offspring and parent for the next generation. DE operators are explained briefly in the following subsections.

3.1. Mutation

A trial vector is generated by the DE mutation operator for each individual of the current population. For generating the trial vector, a target vector is mutated with a weighted differential. An offspring is produced in the crossover operation using the newly generated trial vector. If G is the index for generation counter, the mutation operator for generating a trial vector $u_i(G)$ from the parent vector $x_i(G)$ is defined as follows:

- Select a target vector, $x_{i_1}(G)$, from the population, such that $i\neq i_1$.

- Again, randomly select two individuals, x_{i_2} and x_{i_3}, from the population such that $i \neq i_1 \neq i_2 \neq i_3$.
- Then the target vector is mutated for calculating the trial vector as follows:

$$u_i(G) = x_{i_1}(G) + \underbrace{F \times \overbrace{(x_{i_2}(G) - x_{i_3}(G))}^{\text{Variation Component}}}_{\text{Step size}} \tag{10}$$

where $F \in [0,1]$ is the mutation scale factor which is used for controlling the amplification of the differential variation [42].

3.2. Crossover

Offspring $x'_i(G)$ is generated using the crossover of parent vector, $x_i(G)$ and the trial vector, $u_i(G)$ as follows:

$$x'_{ij}(G) = \begin{cases} u_{ij}(G) & \text{if } j \in J \\ x_{ij}(G) & \text{otherwise.} \end{cases} \tag{11}$$

where J is the set of crossover points or the points that will go under perturbation, $x_{ij}(G)$ is the jth element of the vector $x_i(G)$.

Different methods may be used to determine the set J of crossover points in which binomial crossover and exponential crossover are the most frequently used [42]. In this paper, the DE and its variants are implemented using the binomial crossover where for a D-dimensional problem, the crossover points are randomly selected from the set of possible points, {1, 2, … , D}. Algorithm 1 shows the steps of binomial crossover to generate crossover points [42].

Algorithm 1. Binomial crossover.

Let CR represents the probability with which the considered crossover points will be included.
$U(1,D)$ is a uniformly distributed random integer between 1 and D.
$J = \phi$
$j^* \sim U(1,D)$;
$J \leftarrow J \cup j^*$;
for each $j \in 1 \ldots D$ **do**
  if $U(0,1) < CR$ and $j \neq j^*$ **then**
    $J \leftarrow J \cup j$;
  end if
end for

3.3. Selection

There are two functions for the selection operator: first, it selects the individual for the mutation operation to generate the trial vector, and second, it selects the best, between the parent and the offspring based on their fitness value for the next generation. If fitness of parent is greater than the offspring then parent is selected otherwise offspring is selected:

$$x_i(G+1) = \begin{cases} x'_i(G) & \text{if } f(x'_i(G)) > f(x_i(G)), \\ x_i(G) & \text{otherwise.} \end{cases} \tag{12}$$

This ensures that the population's average fitness does not deteriorate. The pseudo-code for differential evolutionary strategy, is described in Algorithm 2 [42].

Algorithm 2. Differential evolutionary algorithm.

Let F and CR are the control parameters termed as scale factor and crossover probability respectively.
Let P is the population vector.
Initialize the control parameters F and CR;
Create and initialize the population $P(0)$ of NP individuals;
while termination condition **do**
  for each individual $x_i(G) \in P(G)$ **do**
    Evaluate the fitness $f(x_i(G))$;
    Create the trial vector $u_i(G)$ by applying the mutation operator;
    Create an offspring $x'_i(G)$ by applying the crossover operator;
    if $f(x'_i(G))$ is better than $f(x_i(G))$ **then**
      Add $x'_i(G)$ to $P(G+1)$;
    else
      Add $x_i(G)$ to $P(G+1)$;
    end if
  end for
end while
Return the fittest individual as the solution;

4. The proposed DE based segmentation method

The whole process of the proposed strategy is divided into two cascaded DE based segmentation phases as explained in Section 2. The first phase is used for intensity based segmentation and the resultant objects are given as input to subsequent phase for feature based segmentation. The process of each phase is explained as follows:

- *Phase*1: Segmentation of leukocyte type objects from inflamed mice skin images based on intensity of each pixel (for RGB plane).

  1. Initialize parameters, create class centers based on levels as shown in Section 2.1.
  2. Create a population randomly and assign the values of the individuals equal to class centers.
  3. Assign the pixels to the nearest center class based on intensity using fitness function described by Eq. (7).
  4. Generate an offspring from three different parents which are selected randomly.
  5. Select one from the offspring and its parent which has better performance.
  6. Repeat from steps 3 to 5 until termination criteria is not satisfied which is the maximum number of generations.
  7. Select the nucleus and cytoplasm pixels using the calculated thresholds.

- *Phase*2: Segmentation of leukocytes based on feature set.

  1. Initialize parameters, create class centers based on the feature set according to levels as shown in Section 2.2.
  2. Create a population randomly and assign the values of the individuals equal to class centers.
  3. Assign the objects to the nearest center class based on feature set using fitness function described by Eq. (9).
  4. Generate an offspring from three different parents which are selected randomly.
  5. Select one from the offspring and its parent which has better performance.
  6. Repeat from steps 3 to 5 until termination criteria is not satisfied.
  7. Repeat steps 1 to 6 for each feature and generate threshold values for each feature.
  8. Remove the objects having area less than lowest threshold and greater than highest threshold.

9. Remove the objects having feature value more than the highest threshold level for rest of the features.

5. Experimental results

The performance of the proposed two phase segmentation approach using DE has been analyzed by experimenting over inflamed mice skin section images. The setting of parameters for this experiment is discussed below:

- The crossover probability $CR=0.9$ [43].
- The scale factor which controls the implication of the differential variation $F=0.5$.
- Population size $NP=50$.
- The stopping criteria is set to the maximum number of iterations. In this experiment it is set to be 200.

Database of 10 photomicrographs of inflamed mice skin sections stained with routinely used H&E staining method was obtained from Histopathology Section of Defence Research & Development Establishment, Gwalior, India. All the photomicrographs were acquired using DC500 camera (Leica, Germany) attached with DMLB microscope (Leica, Germany) at $40\times$ magnification. All the photomicrographs were subjected to microscopic analysis by three expert pathologists who have manually marked the nuclei in the images. From these marked images common cells were selected for the result analysis.

The representative three photomicrographic images from the database are shown in Fig. 1 along with marked cell images. To see the effect of the number of threshold levels on the accuracy, empirical experiments have been done on the images under consideration. From these experiments, six and five levels of thresholds for intensity and feature based segmentation, respectively, have been selected for the proposed strategy.

The results of the proposed strategy for intensity and feature based segmentation have been presented in Fig. 2. In this figure, representative noisy objects in Fig. 2a and b are shown by circles which have been removed in phase-2. The accuracy of the proposed strategy for both the phases is calculated by dice coefficient (DC) [44] as shown below

$$D(A,B)=\frac{2|A\cap B|}{(|A|+|B|)} \tag{13}$$

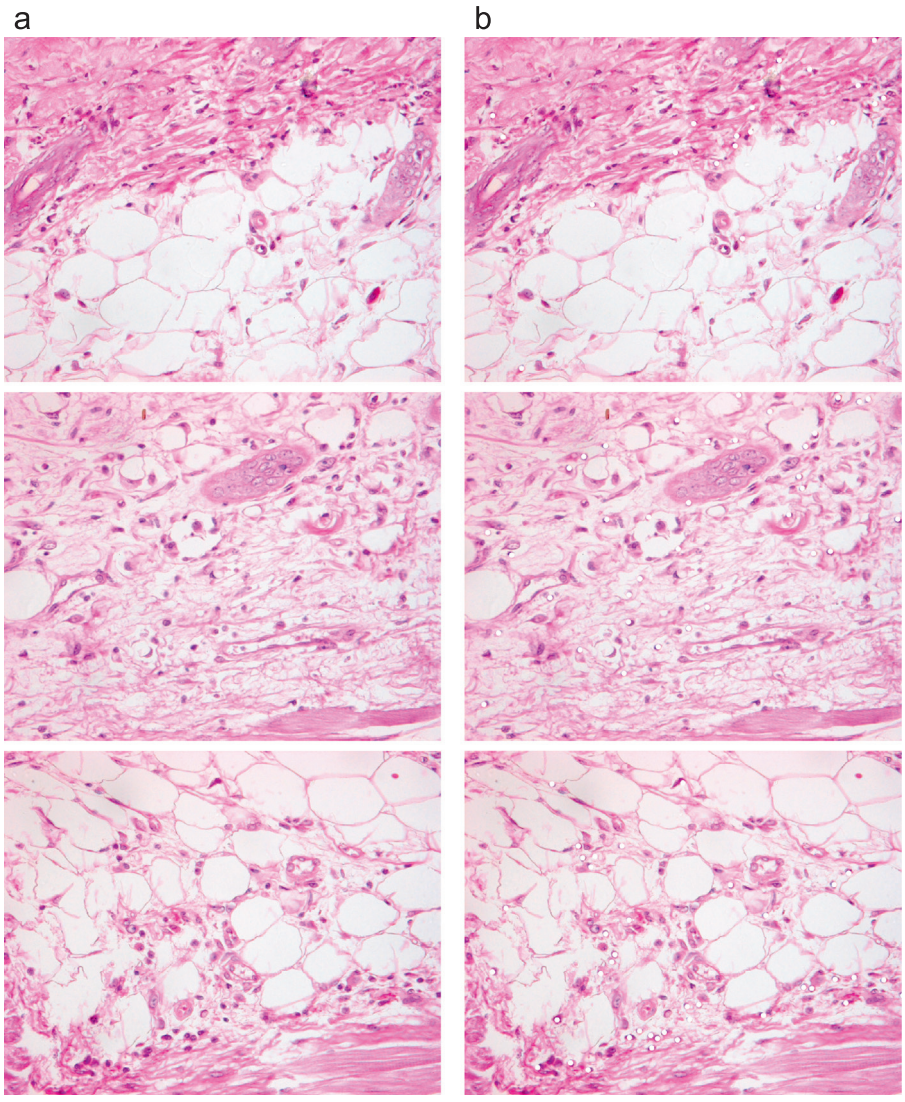

Fig. 1. Representative photomicrographs of inflamed mice skin section stained with H&E staining and acquired at $40\times$: (a) original images and (b) leukocyte marked images.

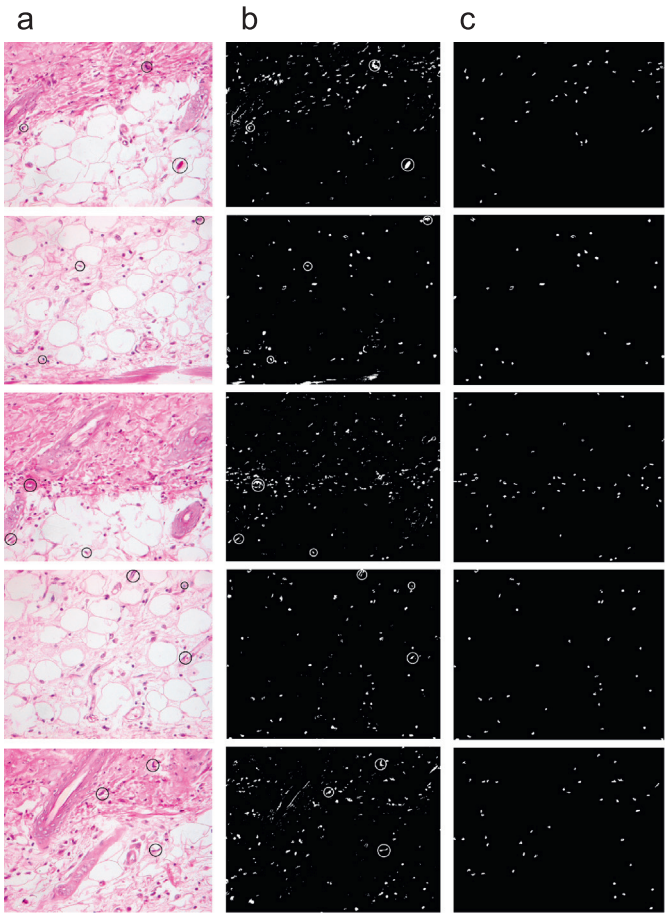

Fig. 2. Representative first five photomicrographs of inflamed mice skin section: (a) original image, (b) intensity based segmented images, (c) feature based segmented images. Circles, drawn in the images a and b, are showing some of the noisy objects which are in phase-1 and removed in phase-2.

Table 1
Accuracy results for each phase of proposed segmentation method in terms of dice coefficient.

Images	Actual cells	Phase-1 results				Phase-2 results			
		TP	FP	FN	DC1	TP	FP	FN	DC2
Image 1	16	15	642	1	0.135336823	12	36	4	0.319089382
Image 2	26	26	247	0	0.344860346	17	12	9	0.469395419
Image 3	22	22	723	0	0.18364499	18	45	4	0.351201784
Image 4	19	19	174	0	0.317200697	16	25	3	0.525019322
Image 5	26	25	654	1	0.233170629	17	26	9	0.417798427
Image 6	30	29	220	1	0.388521479	20	4	10	0.654787182
Image 7	32	23	738	9	0.171957037	21	22	11	0.524970534
Image 8	30	25	364	5	0.244827855	20	14	10	0.541406488
Image 9	43	37	596	6	0.322639395	33	14	10	0.609432509
Image 10	15	14	677	1	0.113552614	11	50	4	0.243819953

where A and B represent the ground truth set of pixels and segmented region of pixels, respectively. For any experiment, the higher value of dice coefficient represents the better segmentation accuracy. Results of dice coefficient for both the phases of the proposed strategy are shown in Table 1. In Table 1, TP represents the number of true positive cells (truly identified cells), FP represents false positive cells (artifacts), FN represents false negative cells (cells which cannot be identified), DC1 represents dice coefficient for phase-1, and DC2 represents dice coefficient for phase-2. It is clear form Table 1 and Fig. 2 that the accuracy of phase-2 images is higher than the phase-1 images as the number of noisy elements have been minimized significantly.

Further, the proposed strategy is compared with the well-known image segmentation techniques named K-means [33], EM algorithm [34], Fuzzy c-means [35] and Otsu's threshold [36]. The pictorial comparison of the first five images is shown in Fig. 3. The results of dice coefficient are shown in Table 2 and Fig. 4. By analyzing the results, it is evident that for the considered image database, the proposed approach gives fewer number of noisy elements with better accuracy as compare to the other methods. To test the significant difference between the proposed strategy and considered algorithms, statistical comparison is carried out for dice coefficient using Student's t-test [45]. In this experiment, Student's t-test is applied for a confidence level of 0.95. Table 3 shows the results of the same test for the null hypothesis that there is no difference in the dice coefficient for 30 runs. In this table, all values consist of '+' which indicates that there are significant differences between proposed strategy and considered existing methods, i.e. the null hypothesis is rejected.

Further, the considered algorithms are compared by their computational efficiency. Let an image is to be segmented, having L gray levels and N number of pixels, using M thresholds. The computational complexity of Otsu's threshold method is $O(L^M)$ for $M \ll L$ as it is an exhaustive method that finds set of all possible thresholds [46]. This complexity exponentially depends on the number of thresholds. The computational complexity of K-means algorithm is $O(M.N.I)$, where I is the number of iterations [46]. The EM algorithm has E-step and M-step which have similar computational complexities of $O(M.N.I)$ [47]. Both the K-means and EM algorithms have linear time complexity. While the time complexity of FCM is $O(N.M^2.I)$ which is quadratic with respect to number of thresholds [48]. The proposed method has used DE for finding M number of thresholds in the histopathological images. Therefore, the runtime complexity of the proposed algorithm is based on stopping criteria, mutation and crossover operations of DE. In each iteration of DE, a loop over NP is performed which contains a loop over M [49]. Since the mutation and crossover operations are performed at the component level for each DE vector, Zielinski et al. [49] investigated that the number of fundamental operations in $DE/rand/1/bin$ are $O(NP.M)$. If there are I number of iterations then the runtime complexity of the algorithm will be $O(NP.M.I)$ which is also linear to the number of thresholds.

For fare comparison, all the considered algorithms are implemented in MatLab 7.9 and tested on the same system environment having Intel Core i5 processor with 2 GB RAM. Table 4 shows the computation time in seconds for all the considered algorithms. It is obvious from Table 4 that for the considered number of thresholds, all other methods are computationally inefficient than the proposed strategy except Otsu's threshold method. But in the tissue image analysis, accuracy is more important than the computational time and it is proved by the DC analysis that the proposed strategy outperforms considered algorithms.

6. Discussion and conclusion

In this work, a novel and efficient strategy is proposed based on DE meta-heuristic for leukocyte segmentation in the images of inflamed mice skin section stained with H&E staining and acquire at 40 × magnification. In the proposed strategy, the segmentation process is divided into two phases namely intensity based segmentation and feature based segmentation. The intensity based segmentation phase extracts the leukocyte type objects from the images based on their pixel intensity. Further, in the feature based segmentation phase efforts are done to minimize

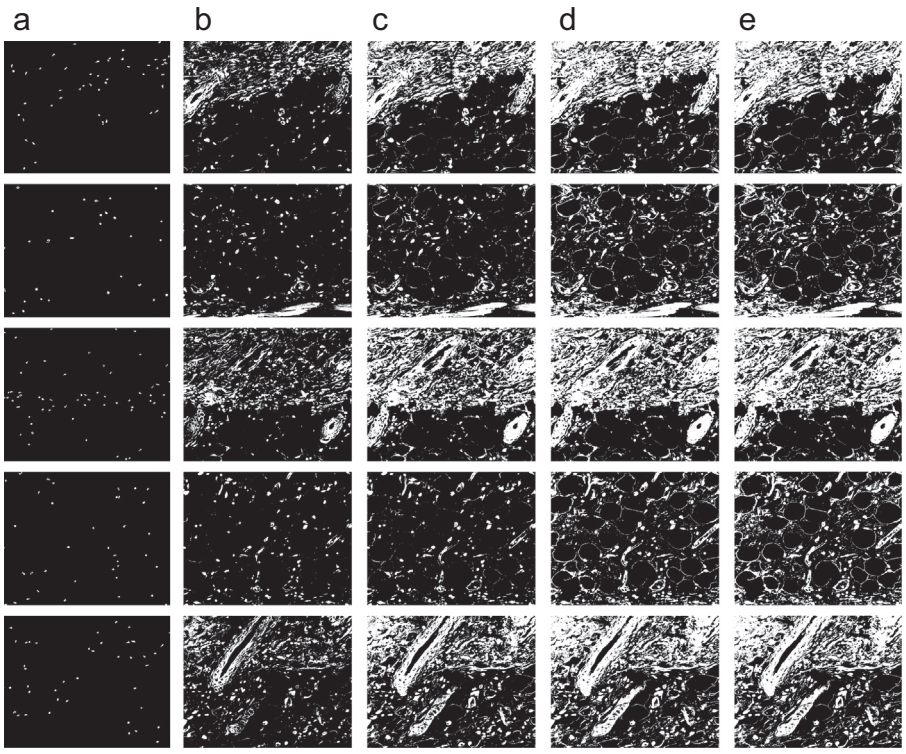

Fig. 3. Representative first five segmented images through (a) proposed method, (b) *K*-means algorithm, (c) EM algorithm, (d) Otsu's threshold, (e) Fuzzy c-mean.

Table 2
Accuracy results for segmentation of leukocytes in terms of dice coefficient.

S. no.	Proposed strategy		EM	Otsu's	*K*-means	Fuzzy
	Phase-1	Phase-2	algorithm	threshold	algorithm	*c*-means
Image 1	0.1353368	0.3190893	0.0134395	0.0108228	0.0271350	0.0038105
Image 2	0.3448603	0.4693954	0.0582134	0.0368524	0.0977403	0.0062537
Image 3	0.183644	0.3512017	0.0154676	0.0131977	0.0331990	0.0052438
Image 4	0.3172006	0.5250193	0.0699182	0.0352622	0.1053839	0.0045304
Image 5	0.2331706	0.4177984	0.0203573	0.0161291	0.0396688	0.0061884
Image 6	0.3885214	0.6547871	0.0647241	0.0379788	0.1051165	0.0073811
Image 7	0.1719570	0.5249705	0.0484280	0.0195185	0.0499123	0.0086406
Image 8	0.2448278	0.5414064	0.0415935	0.0323045	0.0749653	0.0075383
Image 9	0.3226393	0.6094325	0.0429894	0.0353519	0.0851021	0.0099161
Image 10	0.1135526	0.2438199	0.0654581	0.0081695	0.0209197	0.0035783

the noisy elements using four features namely area of cell, eccentricity of cell, ratio of cytoplasm to nucleus area, and solidity of nucleus. With the help of experiments, it is evident that the proposed strategy is better than some commonly used algorithms such as *K*-means, EM algorithm, Fuzzy *c*-means and Otsu's threshold.

The automation of nuclei segmentation is the paramount importance for leukocytes identification system to reduce human workload, individual biasness, and staining variations. Generally, the nuclei segmentation can be categories into threshold based methods [50], deformable models based methods [51] and pattern recognition based methods [52]. Threshold based methods further can be divided into histogram based, edge based and region based techniques. Histogram based techniques have been successfully used for images with uniform illumination. Edge detection algorithms have relied on the idea of detecting discontinuities of pixel intensities at the boundary of different objects. Edge detection and histogram-based methods are most sensitive to the presence of noise and artifacts. Region-based algorithms have assumed objects characterized by homogeneous

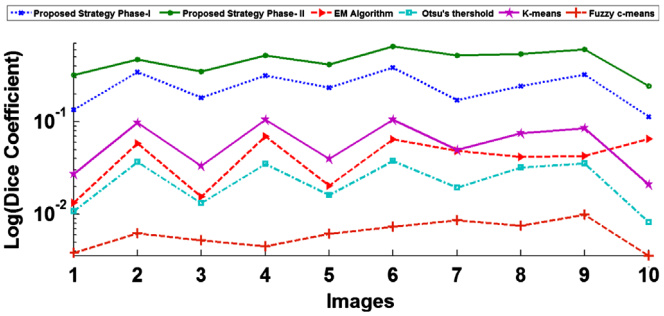

Fig. 4. Comparison of the proposed strategy with *K*-means, Fuzzy *c*-means, EM, and Otsu's threshold methods.

intensity and have performed segmentation utilizing region growing, splitting and merging. However, region-based algorithms are less sensitive to artifacts but have high computational complexity. H&E stained images are considered among the most complex, noisy images and are characterized by great variability

Table 3
Comparison of proposed strategy with existing methods using Student's *t*-test for dice coefficient.

S. no.	Dice coefficient			
	K-means algorithm	Fuzzy *c*-means	EM algorithm	Otsu's threshold
Image 1	+	+	+	+
Image 2	+	+	+	+
Image 3	+	+	+	+
Image 4	+	+	+	+
Image 5	+	+	+	+
Image 6	+	+	+	+
Image 7	+	+	+	+
Image 8	+	+	+	+
Image 9	+	+	+	+
Image 10	+	+	+	+

Table 4
Comparison of proposed strategy with other considered methods in terms of computational time.

S. no.	Computational time in seconds				
	Proposed strategy	*K*-means algorithm	Fuzzy *c*-means	EM algorithm	Otsu's threshold
Image 1	7.9490	10.5288	54.1012	25.8745	1.3004
Image 2	6.9856	9.7568	54.1230	23.5557	1.2866
Image 3	7.0657	10.3758	55.1397	24.4527	1.2931
Image 4	7.0743	10.7607	54.2450	23.3528	1.2888
Image 5	7.0543	10.2543	54.5844	23.9783	1.2934
Image 6	7.7029	10.2357	54.9132	23.5974	1.2920
Image 7	7.5566	10.2555	55.1582	23.6876	1.2942
Image 8	7.9314	10.7451	54.4821	23.6972	1.2930
Image 9	7.9196	10.2567	51.6278	23.4659	1.2895
Image 10	7.2585	10.5192	54.7723	23.3585	1.2966

in staining intensity; thus, the aforementioned segmentation techniques are difficult to implement on H&E images. Contour-based models are considered very promising for automated nuclear segmentation. The success of contour models depends mainly on the initial assumptions made for nuclear morphology, the existence of subnuclear structures and mostly on the initialization condition of the deformable model; the more accurate the initial estimation concerning nuclei boundaries, the better the contour model works. These limitations have restricted the application of active contours in nuclear segmentation of H&E images. Pattern recognition approaches have been established on the basis of supervised training of a classifier to discriminate between nuclei and background.

To overcome the stated problems of classical algorithms for leukocyte segmentation from tissue images, heuristic based algorithms are supposed to be more suitable as they do not require a priori assumptions about size, shape, texture or spatial distribution of leukocytes. Therefore, in the proposed work, differential evolution algorithm is successfully used for segmenting the leukocytes from the inflamed mice skin section images. The obtained results are promising and the proposed strategy requires little parameter settings which makes its implementation easy. The method converges fast to the global optima for any initial parameter values. As per our best knowledge this is the first inline work to segment the leukocytes from complex inflamed mice skin section images using differential evolution algorithm.

A future development of this work will aim to apply DE's advance variants such as JADE, SaDE, DEGL, jDE, MDE_*p*BX, etc., and other advance EAs to segment the leukocytes from the tissue section images and study their accuracies and performances in our framework.

Acknowledgments

Authors are thankful to Defence Research and Development Establishment (DRDE), Gwalior, India, for funding a part of this work under the project (DRDE-P1-2011/Task-190). All the skin section images were obtained from archived animal studies that have a prior approval from the Institutional Animal Ethical Committee of Defence Research & Development Establishment, Gwalior, India. Authors are also thankful to Dr. S.C. Pant, Scientist 'F' at D.R.D.E., Gwalior, Dr. Vinay Lomash, Ph.D., MVSc (Pathology) and Dr. Vikas Galav, MVSc (Pathology) for tendering their valuable help in the analysis of microscopic images for manual leukocyte extraction.

References

[1] S.L. Robbins, V. Kumar, A.K. Abbas, R.S. Cotran, N. Fausto, Robbins and Cotran Pathologic Basis of Disease, WB Saunders Company, 2010.
[2] V. Lomash, S.K. Parihar, N.K. Jain, A.K. Katiyar, Effect of solanum nigrum and ricinus communis extracts on histamine and carrageenan-induced inflammation in the chicken skin, Cellular and Molecular Biology 56 (2010) 1239–1251.
[3] V. Lomash, S.E. Jadhav, F. Ahmed, R. Vijayaraghavan, S.C. Pant, Evaluation of wound-healing formulation against sulphur mustard-induced skin injury in mice, Human and Experimental Toxicology 31 (2011) 588–605.
[4] D.B. Duarte, M.R. Vasko, J.C. Fehrenbacher, Models of inflammation: Carrageenan air pouch, Current Protocols in Pharmacology 1 (2012) 5.6.1–5.6.6.
[5] S.H. Ong, X.C. Jin, Jayasooriah, R. Sinniah, Image analysis of tissue sections, Computers in Biology and Medicine 26 (1996) 269–279.
[6] M.N. Gurcan, L.E. Boucheron, A. Can, A. Madabhushi, N.M. Rajpoot, B. Yener, Histopathological image analysis: a review, IEEE Reviews in Biomedical Engineering 2 (2009) 147–171.
[7] D. Weinland, R. Ronfard, E. Boyer, A survey of vision-based methods for action representation, segmentation and recognition, Computer Vision and Image Understanding 115 (2011) 224–241.
[8] J.L. Raheja, K. Das, A. Chaudhary, An efficient real time method of fingertip detection, in: Proceedings of the Seventh International Conference on Trends in Industrial Measurements and Automation, 2011.
[9] J.L. Raheja, M.B.L. Manasa, A. Chaudhary, S. Raheja, Abhivyakti: Hand gesture recognition using orientation histogram in different light conditions, in: Proceedings of the Fifth International Conference on Artificial Intelligence, 2011.
[10] C. Pan, D. Park, Y. Yang, H. Yoo, Leukocyte image segmentation by visual attention and extreme learning machine, Neural Computing & Applications (2011) 1–11.
[11] N. Theera-Umpon, S. Dhompongsa, Morphological granulometric features of nucleus in automatic bone marrow white blood cell classification, IEEE Transactions on Information Technology in Biomedicine 11 (2007) 353–359.
[12] R. Storn, K. Price, Differential evolution—a simple and efficient heuristic for global optimization over continuous spaces, Journal of Global Optimization 11 (1997) 341–359.
[13] D.E. Goldberg, Genetic Algorithms in Search, Optimization and Machine Learning, Addison-Wesley Longman Publishing Co., Inc., 1989.
[14] K.V. Price, R.M. Storn, J. Lampinen, Differential Evolution: A Practical Approach to Global Optimization, Springer, Berlin, 2005.
[15] S. Das, P.N. Suganthan, Differential evolution: a survey of the state-of-the-art, IEEE Transactions on Evolutionary Computation 15 (2011) 4–31.
[16] J. Zhang, A.C. Sanderson, Jade: adaptive differential evolution with optional external archive, IEEE Transactions on Evolutionary Computation 13 (2009) 945–958.
[17] A.K. Qin, V.L. Huang, P.N. Suganthan, Differential evolution algorithm with strategy adaptation for global numerical optimization, IEEE Transactions on Evolutionary Computation 13 (2009) 398–417.
[18] S. Das, A. Abraham, U.K. Chakraborty, A. Konar, Differential evolution using a neighborhood-based mutation operator, IEEE Transactions on Evolutionary Computation 13 (2009) 526–553.
[19] J. Brest, S. Greiner, B. Boskovic, M. Mernik, V. Zumer, Self-adapting control parameters in differential evolution: a comparative study on numerical benchmark problems, IEEE Transactions on Evolutionary Computation 10 (6) (2006) 646–657.
[20] S.M. Islam, S. Das, S. Ghosh, S. Roy, P.N. Suganthan, An adaptive differential evolution algorithm with novel mutation and crossover strategies for global numerical optimization, IEEE Transactions on Systems, Man, and Cybernetics, Part B: Cybernetics 42 (2012) 482–500.
[21] J. Vesterstrom, R. Thomsen, A comparative study of differential evolution, particle swarm optimization, and evolutionary algorithms on numerical

benchmark problems, in: Proceedings of the IEEE Congress on Evolutionary Computation, 2004.
[22] K. Hammouche, M. Diaf, P. Siarry, A comparative study of various meta-heuristic techniques applied to the multilevel thresholding problem, Engineering Applications of Artificial Intelligence 23 (2010) 676–688.
[23] V. Osuna-Enciso, E. Cuevas, H. Sossa, A comparison of nature inspired algorithms for multi-threshold image segmentation, Expert Systems with Applications. Available online 5 September 2012.
[24] M. Iwan, R. Akmeliawati, T. Faisal, H.M. Al-Assadi, Performance comparison of differential evolution and particle swarm optimization in constrained optimization, Procedia Engineering 41 (2012) 1323–1328.
[25] S. Das, A. Abraham, A. Konar, Automatic clustering using an improved differential evolution algorithm, IEEE Transactions on Systems, Man and Cybernetics, Part A: Systems and Humans 38 (2008) 218–237.
[26] T.T. Nguyen, S. Yang, J. Branke, Evolutionary dynamic optimization: a survey of the state of the art, Swarm and Evolutionary Computation 6 (2012) 1–24.
[27] L. Arya, P. Singh, L. Titare, Optimum load shedding based on sensitivity to enhance static voltage stability using de, Swarm and Evolutionary Computation 6 (2012) 25–38.
[28] P. Rocca, G. Oliveri, A. Massa, Differential evolution as applied to electromagnetics, IEEE Antennas and Propagation Magazine 53 (2011) 38–49.
[29] M. Dehmollaian, Through-wall shape reconstruction and wall parameters estimation using differential evolution, IEEE Geoscience and Remote Sensing Letters 8 (2011) 201–205.
[30] A. Qing, Dynamic differential evolution strategy and applications in electromagnetic inverse scattering problems, IEEE Transactions on Geoscience and Remote Sensing 44 (2006) 116–125.
[31] C.H. Sun, C.C. Chiu, Application of finite-difference time domain and dynamic differential evolution for inverse scattering of a two-dimensional perfectly conducting cylinder in slab medium, Journal of Electronic Imaging 19 (2010) 043016.
[32] C.H. Sun, C.C. Chiua, C.L. Lia, C.H. Huanga, Time domain image reconstruction for homogenous dielectric objects by dynamic differential evolution, Electromagnetics 30 (2010) 309–323.
[33] J.A. Hartigan, M.A. Wong, Algorithm as 136: a *K*-means clustering algorithm, Journal of the Royal Statistical Society. Series C (Applied Statistics) 28 (1979) 100–108.
[34] A.P. Dempster, N.M. Laird, D.B. Rubin, Maximum likelihood from incomplete data via the EM algorithm, Journal of the Royal Statistical Society. Series B (Methodological) 39 (1977) 1–38.
[35] J.C. Bezdek, Pattern Recognition with Fuzzy Objective Function Algorithms, Kluwer Academic Publishers, 1981.
[36] N. Otsu, A threshold selection method from gray-level histograms, Automatica 11 (1975) 285–296.
[37] U. Chakraborty, Advances in Differential Evolution, Springer-Verlag, 2008.
[38] V. Aslantas, M. Tunckanat, Differential evolution algorithm for segmentation of wound images, in: Proceedings of the IEEE International Symposium on Intelligent Signal Processing, 2007.
[39] M.G.H. Omran, A.P. Engelbrecht, A. Salman, Differential evolution methods for unsupervised image classification, in: Proceedings of the IEEE Congress on Evolutionary Computation, 2005.
[40] P. Ghamisi, M. S. Couceiro, N. M. F. Ferreira, L. Kumar, Use of darwinian particle swarm optimization technique for the segmentation of remote sensing images, in: Proceedings of the IEEE International Symposium on Geo Science and Remote Sensing, 2012.
[41] M. Sezgin, B. Sankur, Survey over image thresholding techniques and quantitative performance evaluation, Journal of Electronic Imaging 13 (2004) 146–168.
[42] A. Engelbrecht, Computational Intelligence: An Introduction, Wiley, 2007.
[43] R. Gamperle, S.D. Muller, A. Koumoutsakos, A parameter study for differential evolution, Advances in Intelligent Systems, Fuzzy Systems, Evolutionary Computation 10 (2002) 293–298.
[44] K.H. Zou, S.K. Warfield, A. Bharatha, C. Tempany, M.R. Kaus, S.J. Haker, W.M. Wells, F.A. Jolesz, R. Kikinis, Statistical validation of image segmentation quality based on a spatial overlap index, Academic Radiology 11 (2004) 178–189.
[45] C. Croarkin, P. Tobias, Nist/Sematech e-Handbook of Statistical Methods, 2012. URL Available at: 〈http://www.itl.nist.gov/div898/handbook/〉.
[46] L. Dongju, Y. Jian, Otsu method and *K*-means, in: Proceedings of the International Conference on Hybrid Intelligent Systems, 2009.
[47] T. Hu, S.Y. Sung, A hybrid em approach to spatial clustering, Computational Statistics & Data Analysis 50 (2006) 1188–1205.
[48] P. Hore, L. Hall, D. Goldgof, Single pass fuzzy c means, in: Proceedings of the IEEE International Conference on Fuzzy Systems, 2007.
[49] K. Zielinski, D. Peters, R. Laur, Run time analysis regarding stopping criteria for differential evolution and particle swarm optimization, in: Proceedings of the International Conference on Exp./Process/System Modelling/Simulation/Optimization, 2005.
[50] N. Malpica, C. Ortiz de Solorzano, J.J. Vaquero, A. Santos, I. Vallcorba, J.M. Garcia-Sagredo, F. del Pozo, Applying watershed algorithms to the segmentation of clustered nuclei, Cytometry 28 (1997) 289–297.
[51] D. Glotsos, P. Spyridonos, D. Cavouras, P. Ravazoula, P.A. Dadioti, G. Nikiforidis, Automated segmentation of routinely hematoxylin–eosin-stained microscopic images by combining support vector machine clustering and active contour models, Analytical and Quantitative Cytology and Histology 26 (2004) 331–340.
[52] A. Jalba, M. Wilkinson, J. Roerdink, Automatic image segmentation using a deformable model based on charged particles, Image Analysis and Recognition 3211 (2004) 1–8.